ISSN 0036-0244, Russian Journal of Physical Chemistry A, 2024, Vol. 98, No. 14, pp. 3433–3441. © Pleiades Publishing, Ltd., 2024.

XXIV INTERNATIONAL CONFERENCE ON CHEMICAL THERMODYNAMICS IN RUSSIA (RCCT-2024)

Study of Sorption Capacity of Zeolite Catalysts to Glycerol by Thermal Analysis and Calorimetry

I. A. Zvereva[a,*] (ORCID: 0000-0002-6898-3897), M. G. Shelyapina[b] (ORCID: 0000-0003-3769-941X), I. A. Minich [c] (ORCID: 0000-0003-0183-2290), Y. A. Anufrikov[c], O. I. Silyukov[a] (ORCID: 0000-0003-1235-727X), A. Samadov[a] (ORCID: 0000-0003-0016-0760), A. I. Neupokoev[a], G. A. Valkovskiy[b] (ORCID: 0000-0002-5651-8234), and V. Petranovskii[d] (ORCID: 0000-0002-8794-0593)

[a] *Institute of Chemistry, St. Petersburg State University, St. Petersburg, 199034 Russia*

[b] *Department of Nuclear Physics Research Methods, St. Petersburg State University, St. Petersburg, 199034 Russia*

[c] *Centre for Thermal Analysis and Calorimetry, St. Petersburg State University, St. Petersburg, 199034 Russia*

[d] *Center for Nanoscience and Nanotechnology, National Autonomous University of Mexico, Ensenada, B.C., Mexico*

** e-mail: irina.zvereva@spbu.ru*

Received August 20, 2024; revised August 20, 2024; accepted September 10, 2024

Abstract—This work presents the results of the study of glycerol and water sorption using two complimentary approaches, simultaneous thermal analysis and isothermal sorption calorimetry, on zeolites differing in the framework topology and post modifications (natural clinoptilolite, protonated zeolite ZSM-5 with Si/Al ratio of 50, commercial Na-mordenite with Si/Al ratio of 6.5 then modified by ion exchange for copper ions, or by alkaline etching to develop mesoporosity, and pillared mordenite). For the studied mordenites a correlation between texture and composition and sorption capacity towards glycerol and water was shown. Analysis of glycerol and water desorption suggests the optimal temperature range for catalytic conversion of glycerol via dehydration and carboxylation.

Keywords: zeolite, mordenite, ZSM-5, clinoptilolite, glycerol, sorption, thermal analysis, calorimetry

DOI: 10.1134/S003602442470300X

INTRODUCTION

A steady growth in the production of biofuels from biomass waste has led to a sharp increase in the output of crude glycerol, the main by-product (about 10 wt %) of the biodiesel industry [1]. The overproduction of crude glycerol reduces its economic value and creates environmental problems because it cannot be utilized in the environment. From these perspectives the effective use of crude glycerol is crucial for the viability and sustainability of biodiesel production. The need for effective technologies to utilize a huge amount of by-products of biodiesel production requires the development of crude glycerol recycling methods, which would help reduce society's dependence on non-renewable resources and promote the development of integrated biorefineries [2]. Being a very attractive "green" building block, glycerol can be converted into value-added products [3–5] through transesterification [5, 6], dehydration [7, 8], carboxylation [9, 10], synthesis of aromatic compounds [11] and other reactions [12].

For all processes of catalytic conversion of glycerol, the sorption characteristics of the catalyst are of great importance, namely, high sorption capacity with respect to glycerol and low sorption capacity with respect to reaction products. In particular, the processes of glycerol dehydration to acrolein or acetol [7, 8], or glycerol carboxylation to form glycerol carbonate [9, 10], which are in high demand in various fields of chemical industry, are accompanied by water formation that must be removed. The removal of water can be accomplished by the addition of various highly hydrophilic substances such as acetonitrile, methanol [13, 14] or sorbents [15], which further complicates the separation of the target products.

In this regard, when developing efficient catalysts for glycerol conversion, it is necessary to investigate the glycerol sorption processes, primarily the glycerol sorption capacity, as well as the kinetic and thermodynamic characteristics of adsorption/desorption processes. Moreover, it is important to study the sorption properties of the catalyst towards water, as it is desirable to choose a catalyst if not hydrophobic, then at least with a low sorption capacity with respect to water. It should be noted that, unlike water sorption on catalysts that has been studied in sufficient details [16–21],

very little attention has been paid to the study of glycerol sorption [22–24], despite the obvious importance of this phenomenon and its effect on the results of the catalytic process.

Here we present the results of screening zeolites as a support for the design of efficient catalysts for glycerol dehydration and carboxylation. Synthetic microporous zeolites with different framework topologies (mordenite and ZSM-5), mordenite modified with copper, mordenites with mesoporosity introduced by different methods, and natural clinoptilolite were investigated.

The study of the sorption of glycerol and water was carried out by two methods: simultaneous thermal analysis (STA), which combines thermogravimetric analysis (TGA) and differential scanning calorimetry (DSC) of the desorption process, in the temperature range of 30–1000°C, and isothermal sorption calorimetry (ISC) at a temperature of 30°C.

EXPERIMENTAL MATERIALS AND METHODS

Synthesis of the Samples

The series of zeolites studied included six samples: sodium mordenite supplied by Zeolist Int. (Product CBV10A), with a nominal Si/Al atomic ratio equal to 6.5, labelled as NaMOR (code MOR according to the International Zeolite Association (IZA) nomenclature), copper-exchanged mordenite (CuMOR), mordenite with an increased content of mesopores (MOR-meso), pillared mordenite (MOR-P), protonated zeolite ZSM-5 supplied by ZEOCHEM, Switzerland with nominal Si/Al atomic ratio equal 50 (code MFI according to IZA nomenclature), and natural clinoptilolite.

Copper-modified CuMOR sample was prepared according to the method described in [25], which includes the treatment of 0.5 g of the parent NaMOR mordenite in 20 ml of 0.05 M aqueous solution of copper sulfate $CuSO_4$ (99.9%, AO Vecton), which corresponds to a twofold excess of the amount of copper in solution over the calculated ion exchange capacity of NaMOR. The treatment was carried out under stirring, at room temperature (20–25°C), for 12 h. The exchange process was repeated six times to increase the copper content. After that, the samples were filtered, washed with distilled water and dried at room temperature for 12 h.

To prepare mesoporous mordenite MOR-meso, synthetic zeolite NaMOR was treated with 0.2 N aqueous NaOH solution (>98%, AO Vecton) under stirring with a magnetic stirrer, at a temperature of 60°C, for 1 hour. After that, the suspension was cooled in an ice bath, filtered, washed with distilled water, after which the sample was calcined in a vacuum cabinet at 120°C for 2 h.

Pillared mordenite MOR-P was obtained by multistep synthesis procedure according to the method of Ref. [26]: (1) organic components (5.004 g of cetyltrimethylammonium bromide (CTAB), 0.833 g of polyethylene glycol (PEG 20000) and 0.75 g of NaOH were completely dissolved in 58.1 mL of H_2O. After that 34.33 g of sodium silicate solution (25 wt % of SiO_2 and 10.6 wt % of Na_2O) was added. The resulting mixture was stirred for 20 min. Then, the solution of sodium aluminate (0.77 g of $NaAlO_2$ dissolved in 42.6 g of H_2O) was added dropwise. Then, 41.6 g of a 10 wt % H_2SO_4 solution was added under vigorous stirring. The resulting mixture was heated at a temperature of 150°C for 4 days in a Teflon-coated steel autoclave under autogenous pressure. The samples were then filtered, washed with distilled water, then with methanol in a reflux refrigerator for 12 h at 60°C to remove physically clogged surfactants. (2) 1.0 g of the sample obtained in the first step was stirred in 10 g of tetraethoxysilane (TEOS) for 12 h at 25°C, then the sample was filtered and dried at 35°C for 12 h. (3) To hydrolyze TEOS, 2.0 g of the sample was stirred in 20.0 g of distilled water at 90°C for 12 h, after that the sample was washed with distilled water, filtered, and dried at 120°C. (4) To remove organics, the sample obtained after hydrolysis was calcined at 550°C for 4 h in air.

Natural clinoptilolite was taken from the San Luis Potosi deposit, Mexico. According to the phase analysis data reported previously [27] it contains 92% of clinoptilolite phase and 8% of quartz.

Characterization of the Samples

To confirm the crystal structure, the prepared samples were characterized by X-ray diffraction (XRD) on a Bruker D8 DISCOVER diffractometer. Sample morphology and elemental composition were studied by scanning electron microscopy (SEM) and energy dispersive X-ray spectroscopy (EDS) using a Zeiss Merlin microscope equipped with an Oxford Instruments INCAx-act EDX console and an energy dispersive X-ray fluorescence spectrometer Shimadzu EDX 800 HS. The analysis of the specific surface area and porosity was carried out by nitrogen porosimetry using a Quadosorb SI device. Before analysis, the samples were degassed under vacuum for 6 hours at a temperature of 300°C.

Studies of Sorption by Thermal Analysis Methods

For the STA studies, 60 mg of the zeolite under study pre-calcined at a temperature of 550°C was mixed with 2 ml of glycerol dehydrated at 100°C in an Eppendorf tube of 2 mL, the resulting suspension was stirred using a vortex for 1 min. This was followed by ultrasonic treatment using a non-contact Hielscher ultrasonic homogenizer at 25% intensity for 10 min,

after that the suspension was kept in Eppendorf at room temperature for 5 days, followed by centrifuging. Excess glycerol was separated by decantation and the samples were kept on filter paper for an hour. A probe of 5–10 mg was taken from the sample thus obtained and placed in the crucible of the device to study the process of glycerol desorption. The studies were carried out on a NETZSCH STA 409C/CD device (Germany) in the temperature range of 30–1000°C at a heating rate of 20°C/min in an air atmosphere.

To study the sorption of water, 15–40 mg of the studied zeolite, pre-calcined at a temperature of 550°C, was kept in a desiccator in a humid atmosphere for 40 h, a probe of 5–10 mg was taken and placed in the crucible of the device for studying the process of thermal desorption of water. The studies were carried out on a NETZSCH TG 209 F1 Libra device (Germany) in the temperature range of 30–950°C at a heating rate of 10°C/min in an air atmosphere.

Studies of Sorption by Isothermal Calorimetry

The studies were carried out using a Setaram C80 calorimeter (France), equipped with two cells, which allows simultaneous study of two processes, glycerol sorption and water sorption. The experiment provides a direct access to measure the enthalpy characteristic of the sorption of glycerol and water, as well as to obtain indirect conclusions about the kinetics of sorption by the time of reaching the baseline.

Collapsible cells were used for measurements. Each of the cells with a total volume of 6 ml consists of upper and lower spaces, which at the beginning of the experiment are separated by a membrane, which
1 makes it possible to isolate the wetted material (zeolite) from the liquid component (water or glycerol). During the experiment, 8 mg of a zeolite sample was placed in the lower space of each of the cells. The upper space of one of them was filled with glycerol, and the other with water. Next, the cells were placed in a calorimeter thermostat until thermodynamic equilibrium was established at a temperature of 30°C, which was evidenced by a horizontal baseline.

Once equilibrium was established, the cell membranes were alternately destroyed using a striker and a calorimetric signal was recorded in units of a heat flow sensor. The integration of the peak and the use of the conversion factor obtained from calibration to the Joule effect allowed us to obtain the value of the enthalpy effect of glycerol and water sorption for each of the zeolite samples.

RESULTS AND DISCUSSION

XRD, Porosity, Texture and Composition

XRD analysis of the mordenite samples before and after various treatments confirms that all the samples keep the mordenite crystalline structure. The XRD patterns of the starting NaMOR, ion-exchanged CuMOR, and etched in alkali MOR-meso samples are plotted in Fig. 1. It is clearly seen that the both post-synthesis modifications do not strongly affect the XRD pattern, all the mordenite peaks are present, no peaks corresponding to additional phases are not observed (according to our previous studies, ion exchange in copper sulphate solution may result in the formation on additional antlerite phase [28]). Figure 1 also shows the XRD patterns of the MOR-P sample, and the small angle range is shown separately to confirm the formation of lamellar phase. A broad peak at about 2.0 2θ degrees corresponds to reflection from mordenite layers ordered along the *c* axis with an interlayer spacing about $d = 4$ nm [26] with partial disordering, which is confirmed by SEM studies (Fig. 2). Complete XRD pattern presented of the MOR-P sample shows characteristic peaks for the corresponding three-dimensional mordenite. Thus, the sample consists of layers of mordenite separated by pillars of amorphous SiO_2 [26]. XRD pattern of the commercial ZSM-5 can be found anywhere [29]. The X-ray phase analysis of the natural clinoptilolite was reported in our previous study [27].

SEM images shown in Fig. 2 provide information on size and morphology of particles; it is useful to determine particle size, shape, and surface texture. Figures 2(a) and 2(b) for initial mordenite and for mordenite after ion exchange with Cu ions show minimal differences, indicating the absence of dissolution or etching of initial mordenite crystals in neutral solutions. On the contrary, for the MOR-meso sample (Fig. 2c), after alkaline etching, the disappearance of the smallest fractions is observed, and individual single particles with clearly visible transitions between them appear more visibly. The pillared sample (Fig. 2d) shows particles of significantly smaller size, with no visible morphological features. Finally, ZSM-5 zeolites (Fig. 2e) and clinoptilolite (Fig. 2f) exhibit typical bar-shaped and tabular crystals, respectively. The crystal sizes for ZSM5 lie in the range of 0.5–1 μm, and for clinoptilolite about 0.5 μm.

The Si/Al ratio for the studied samples is listed in Table 1. One can see that for the commercial samples it slightly differs from the nominal one. The treatment of mordenite in $CuSO_4$ solution allows us to achieve $Cu/Al = 0.3$, that corresponds to 60% of possible Cu^{2+} ion exchange capacity [28], but does not affect much the Si/Al ratio, while alkali treatment results in a noticeable leaking of silicon. For the pillared MOR-P sample, it should be noted, that this ratio do not characterizes only the zeolite part of the sample, but involves the amorphous SiO_2 pillars as well.

Results of the N_2 adsorption/desorption studies of the zeolite samples are summarized in Table 1. The specific surface area of the samples was determined by a widely used Brunauer–Emmett–Teller (BET)

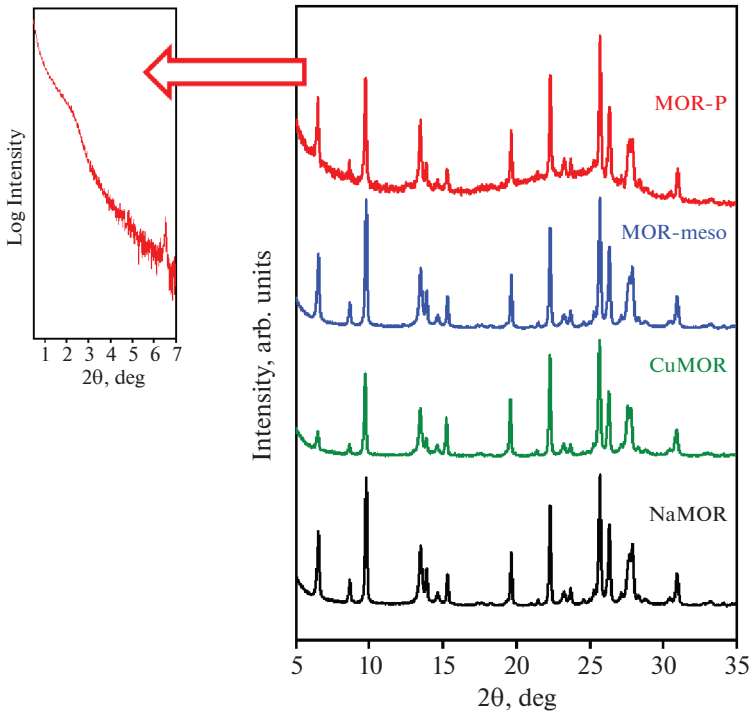

Fig. 1. XRD patterns for NaMOR, CuMOR, MOR-meso and for MOR-P samples; top left: small angle range for MOR-P.

method. Pore sizes and pore volume were determined using the Barrett–Joyner–Halenda (BJH) method.

Samples of the initial synthetic zeolites, NaMOR and ZSM-5, show a surface area typical for microporous zeolites. Copper treatment slightly reduces the porosity of mordenite, but not significantly. For samples with artificially created mesoporosity, the surface area increases markedly, especially for the pillared MOR-P sample, simultaneously it demonstrates a noticeable increase in pore volume (while all the samples exhibit presence of mesoporosity with pore size close to 4 nm, for all the samples except MOR-P, its contribution to the overall pore volume is not very significant).

Table 1. Textural properties of the studied samples, S – specific surface area, V – pore volume, D – pore diameter

Sample	S, m^2/g	V, cm^3/g	D, nm	Si/Al
NaMOR	386	0.08	4.6	5.8
CuMOR	352	0.07	4.7	5.7
MOR-meso	460	0.1	4 & wide distribution of mesopores	1.3
MOR-P	680	0.55	3.5	9
ZSM-5	348	0.03	4.2	54
CLI	120	0.06	4 & wide distribution of mesopores	4.5

Glycerol and Water Desorption

Figure 3 shows the results of thermal analysis of samples placed in glycerol for 5 days. All the studied samples demonstrate significant weight loss during desorption, accompanied by endothermic effects, which indicates a sufficiently high sorption capacity with respect to glycerol. At the same time, natural clinoptilolite demonstrates much lower sorption capacity (weight loss of 29%), which is consistent with its smaller specific surface area (see Table 1). The highest sorption is observed for CuMOR (mordenite modified with copper) and pillared mordenite MOR-P samples, with a mass loss of 74 and 77%, respectively. An important finding is the established optimal temperature range for reactions involving glycerol sorbed on zeolite. Considering that glycerol desorption begins already at 150°C, and at 200°C the desorption of about 50% of glycerol is observed, it can be stated that the preferred temperature for catalytic processes is the interval up to 200°C.

For all the zeolite samples studied, except for natural clinoptilolite, the second step of mass loss at high temperatures in the region above 250°C is observed. The contribution of the second step to the total mass loss is about 5–8.5% (Table 2), which may be due to

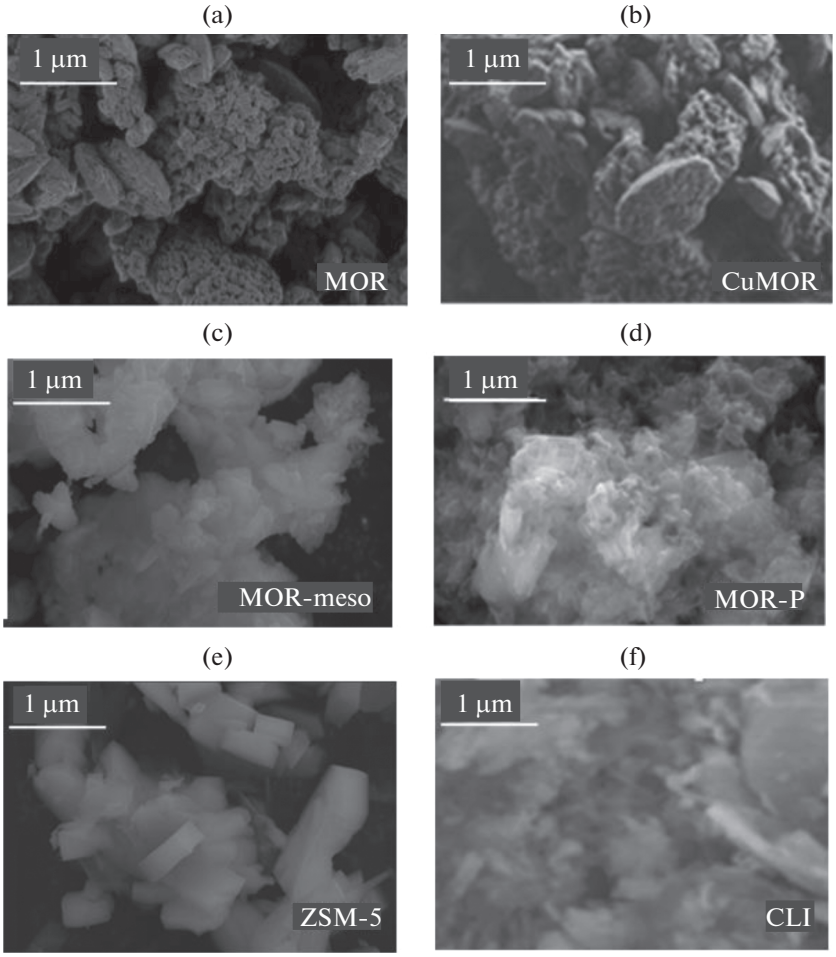

Fig. 2. SEM images of the studied samples: (a) NaMOR, (b) CuMOR, (c) MOR-meso, (d) MOR-P, (e) ZSM-5, (f) CLI.

desorption from the pores. For zeolites with mordenite structure, a correlation between the mass loss upon dehydration and the textural properties of the corresponding zeolites is observed, namely, the highest contribution (8.5 and 6.7%) is observed for the initial NaMOR and copper-modified CuMOR mordenites with smaller surface area (386 and 352 m^2/g), while the smaller contribution (4.6%) is observed for the pillared mordenite MOR-P with the largest surface area (680 m^2/g). This fact can become an experimental basis for further research in order to obtain an information on steric and energetic aspects of the interaction between glycerol molecules and zeolites with different porosity.

The results of thermogravimetric analysis of hydrated samples, shown in Fig. 4, demonstrate a significant difference between zeolite ZSM-5, which practically does not adsorb water, and other studied samples. The hydrophilicity increases in the following series: ZSM-5 ≪ CLI ≪ MOR-meso < NaMOR < CuMOR < MOR-P. It is important that the desorption of water begins much earlier than glycerol, in the range of 100–150°C 50% desorption is observed, by 300°C zeolites almost completely lose water. Based on this, it can be concluded that the most suitable temperature range is 150–200°C, when glycerol is desorbed slightly while water to a large extent.

Glycerol and Water Sorption

The results of a calorimetric study of glycerol and water sorption are shown in Fig. 5 and Table 2. Significant exothermic thermal effects during glycerol sorption are demonstrated by samples of pillared mordenite MOR-P, ZSM-5 and CuMOR, for which the enthalpy of sorption is −80, −59 and −36 J per 1 g of glycerol, respectively. These results correlate with the results of synchronous thermal analysis of glycerol desorption (Fig. 3). Moreover, it should be noted that the ZSM-5 sample is hydrophobic, as evidenced by the enthalpy of water sorption of +1 J/g, which is quite consistent with the results of thermogravimetric analysis: compared to the other samples studied, ZSM-5 exhibits the lowest mass loss upon dehydration (Fig. 4).

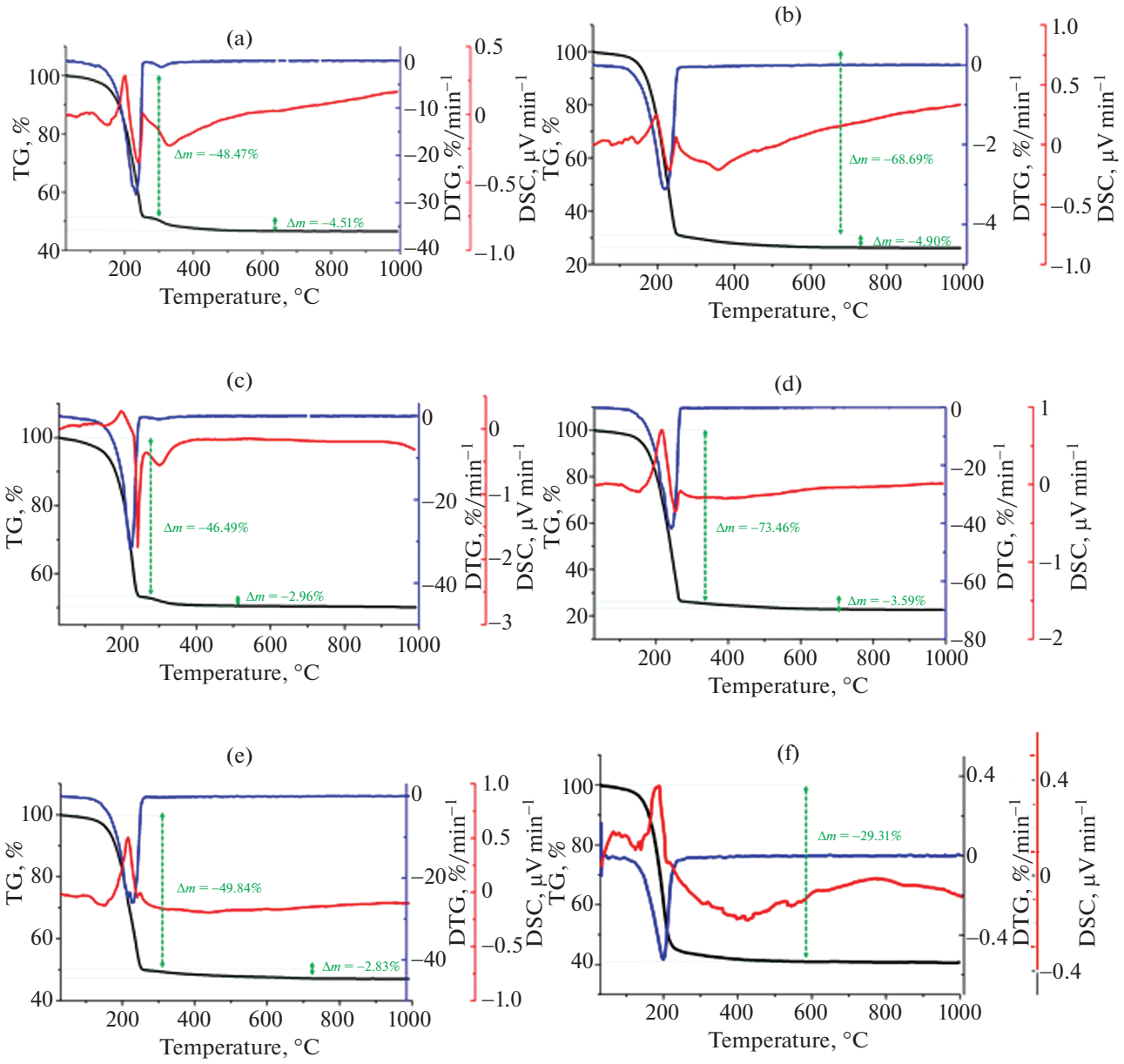

Fig. 3. TG, DTG and DSC curves for glycerol release from the studied samples: (a) NaMOR, (b) CuMOR, (c) MOR-meso, (d) MOR-P, (e) ZSM-5, (f) CLI.

Table 2 shows the thermal effects (enthalpy) of glycerol sorption and mass loss upon glycerol desorption. These data are sufficiently informative to evaluate the sorption capacity of potential zeolite-based catalysts with respect to glycerol. The analysis of these data shows that, firstly, for all samples glycerol sorption is an energetically favorable process (enthalpy of sorption is negative), and therefore, a large amount of glycerol is sorbed at a sufficiently large surface area (>250 m^2/g), which is a favorable factor for glycerol conversion processes on the surface of catalysts. Combining the data of TG and isothermal sorption calorimetry, the thermal effect per mole of sorbed substance was recalculated, which facilitates the comparison of the data in terms of the sorption capacity of zeolite samples with respect to glycerol and water. The molar thermal effect of glycerol sorption for NaMOR, CuMOR and MOR-meso is comparable to the thermal effect of water sorption, for natural clinoptilolite CLI the effect of water sorption is significantly higher. For the pillared mordenite MOR-P и ZSM-5 the glycerol sorption is much more profitable than water. From this point of view, ZSM-5, been hydrophobic as noted above, is the most advantageous compared to other zeolites studied.

Table 2. Results of the study of the sorption of glycerol and water by isothermal calorimetry (ΔH_S – sorbtion enthalpy) and thermogravimetry (Δm – mass loss)

Sample	Glycerol sorbtion					Water sorbtion		
	ΔH_S, J/$g_{zeolite}$	Δm, %			ΔH_S,[a] kJ/mol_{gl}	ΔH_S, J/$g_{zeolite}$	Δm, %	ΔH_S, kJ/mol_{H_2O}
		Total	Step 2	Contribution of Step 2 to total Δm				
NaMOR	–8	53	4.51	8.5	–0.64	–4	11.03	–0.58
CuMOR	–36	73	4.90	6.7	–1.20	–7	12.32	–0.92
MOR-meso	–14	50	2.96	5.9	–1.29	–79	9.74	–1.44
MOR-P	–80	77	3.59	4.6	–2.21	–73	28.11	–0.05
ZSM-5	–59	53	2.83	5.3	–4.78	1	2.24	0.79
CLPL	–11	29	—	—	–2.48	–47	7.60	–11.23

[a] *gl* – glicerol

All methods of mordenite surface modification give an increase in the energy effect of glycerol sorption by 2–3 times. In addition, the calorimetric experiment shows that the process of glycerol sorption to saturation proceeds rather quickly (in 20–30 min), which is also important for the practical use of the catalyst.

Thus, from the point of view of sorption capacity with respect to glycerol, the chosen directions of mordenite modification with copper cations, introduction of mesoporosity (both by alkali treatment and pillaring), as well as the use of protonated ZSM-5 zeolite with a rather high Si/Al ratio, which is more hydrophobic than studied mordenites are promising ways to obtain effective catalysts for glycerol conversion processes.

CONCLUSIONS

In this work on the base of data obtained by thermogravimetry and calorimetry of sorption, a comparative study of sorption and desorption processes of glycerol and water on natural clinoptilolite, protonated ZSM-5 zeolite with Si/Al ratio of 50, commercial sodium mordenite with Si/Al ratio of 6.5 (pristine and modified by copper ion exchange or alkaline etching to develop mesoporosity), and synthesized pillared mordenite with ordered mesopore structure was carried out. A correlation between the texture and composition of mordenite and its sorption capacity

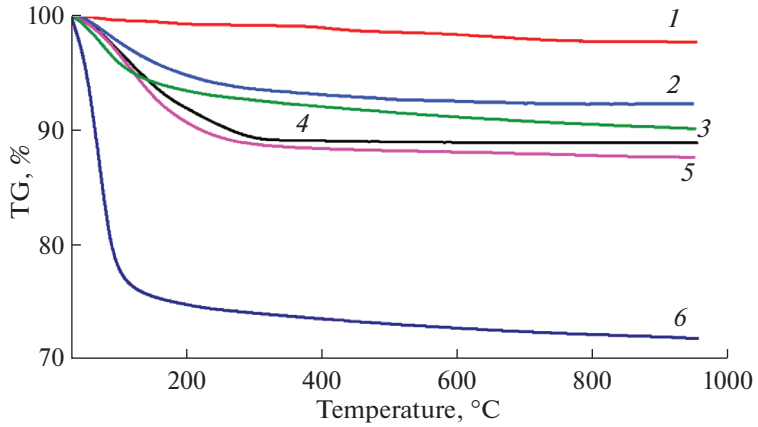

Fig. 4. TG curves for water release from the studied samples: *1* – ZSM-5, *2* – CLI, *3* – MOR-meso, *4* – NaMOR, *5* – CuMOR, *6* – MOR-P.

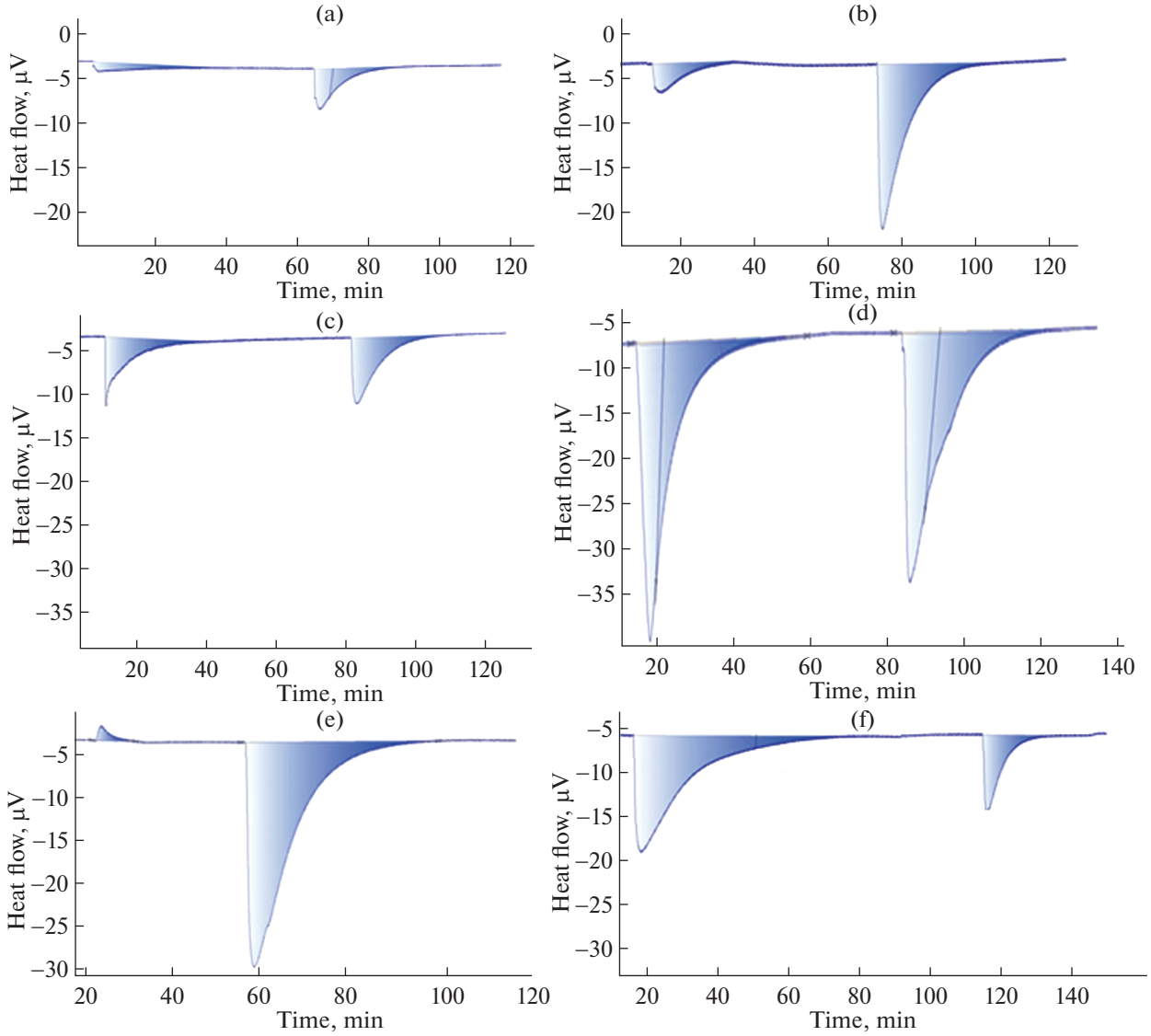

Fig. 5. Thermal effect of glycerol sorption (right) and water sorption (left) for the studied samples: (a) NaMOR, (b) CuMOR, (c) MOR-meso, (d) MOR-P, (e) ZSM-5, (f) CLI.

towards glycerol and water is demonstrated. Based on the analysis of the intervals of desorption of glycerol and water, the conclusion about the optimal temperature range for catalytic conversion of glycerol was made.

ACKNOWLEDGMENTS

The study was conducted using the equipment of the Saint Petersburg State University Research Park: Centre for X-ray Diffraction Studies, Interdisciplinary Centre for Nanotechnology, Centre for Thermal Analysis and Calorimetry, Center for Diagnostics of Functional Materials for Medicine, Pharmacology and Nanoelectronics, Center for Innovative Technologies of Composite Nanomaterials.

FUNDING

The research was supported by Ministry of Education and Science of Russia (grant no. 075-15-2023-611) and DGAPA-PAPIIT Grant IG101623.

CONFLICT OF INTEREST

The authors declare that the research was conducted in the absence of any commercial or financial relationships that could be construed as a potential conflict of interest.

REFERENCES

1. N. Yadav, G. Yadav, and M. Ahmaruzzaman, Ind. Crops. Prod. **210**, 117999 (2024). https://doi.org/10.1016/j.indcrop.2023.117999

2. S. M. Ioannidou, C. Pateraki, D. Ladakis, et al., Bioresour. Technol. **307**, 123093 (2020). https://doi.org/10.1016/j.biortech.2020.123093
3. F. Aprialdi, D. Mujahidin, and G. T. Kadja, Waste Biomass Valor. **15**, 5069 (2024). https://doi.org/10.1007/s12649-024-02487-3
4. I. Zahid, M. Ayoub, and M. H. Nazir, Biomass. Bioenergy **181**, 107029 (2024). https://doi.org/10.1016/j.biombioe.2023.107029
5. V. Aomchad, A. Cristofol, F. Della Monica, et al., Green Chem. **23**, 1077 (2021). https://doi.org/10.1039/d0gc03824e
6. S. Nomanbhay, M. Y. Ong, K. W. Chew, et al., Energies **13**, 1483 (2020). https://doi.org/10.3390/en13061483
7. F. F. Barbosa and T. P. Braga, ChemCatChem **15**, e202200950 (2023). https://doi.org/10.1002/cctc.202200950
8. S. Basu and A. K. Sen, ChemBioEng Rev. **8**, 633 (2021). https://doi.org/10.1002/cben.202100009
9. S. Lukato, G. N. Kasozi, B. Naziriwo, and E. Tebandeke, Curr. Res. Green Sustain. Chem. **4**, 100199 (2021). https://doi.org/10.1016/j.crgsc.2021.100199
10. H. Li, C. Xin, X. Jiao, et al., J. Mol. Catal. A **402**, 71 (2015). https://doi.org/10.1016/j.molcata.2015.03.012
11. S. He, K. Zuur, D. S. Santosa, et al., Appl. Catal. B **281**, 119467 (2021). https://doi.org/10.1016/j.apcatb.2020.119467
12. P. Koranian, Q. Huang, A. K. Dalai, and R. Sammynaiken, Catalysts **12**, 897 (2022). https://doi.org/10.3390/catal12080897
13. H. Li, D. Gao, P. Gao, et al., Catal. Sci. Technol. **3**, 2801 (2013). https://doi.org/10.1039/C3CY00335C
14. J. George, Y. Patel, S. M. Pillai, and P. Munshi, J. Mol. Catal. Chem. **304**, 1 (2009). https://doi.org/10.1016/j.molcata.2009.01.010
15. N. Ozbay, N. Oktar, G. Dogu, and T. Dogu, Ind. Eng. Chem. **51**, 8788 (2012). https://doi.org/10.1021/ie201720q
16. G. L. Catuzo, C. V. Santilli, and L. Martins, Catal. Today **381**, 215 (2021). https://doi.org/10.1016/j.cattod.2020.07.008
17. C. X. A. Da Silva, V. L. C. Gonalves, and C. J. A. Mota, Green Chem. **11**, 38 (2009). https://doi.org/10.1039/b813564a
18. T. E. Souza, I. D. Padula, and M. M. G. Teodoro, Catal. Today **254**, 83 (2015). https://doi.org/10.1016/j.cattod.2014.12.027
19. E. A. Krylova, M. G. Shelyapina, P. Nowak, et al., Microporous Mesoporous Mater. **265**, 132 (2018). https://doi.org/10.1016/j.micromeso.2018.02.010
20. M. Zheng and B. C. Bukowski, ChemRxiv (2024). https://doi.org/10.26434/chemrxiv-2023-pg96c-v3
21. Q. Liu and J. A. van Bokhoven, Chem. Soc. Rev. **53**, 3065 (2024). https://doi.org/10.1039/D3CS00404
22. S. Liu, S. R. Musuku, S. Adhikari, and S. Fernando, Environ. Technol. **30**, 505 (2009). https://doi.org/10.1080/09593330902803019
23. Y. C. Yin, X. Sang, X. F. Xu, et al., Microporous Mesoporous Mater. **294**, 109919 (2019). https://doi.org/10.1016/j.micromeso.2019.1099
24. M. G. Shelyapina, E. P. Maksimova, and A. V. Egorov, J. Struct. Chem. **65**, 574 (2024). https://doi.org/10.1134/S0022476624030120
25. Y. M. Zhukov, M. G. Shelyapina, I. A. Zvereva, et al., Microporous Mesoporous Mater. **259**, 220 (2018) https://doi.org/10.1016/j.micromeso.2017.10.013
26. M. G. Shelyapina, R. I. Yocupicio-Gaxiola, I. V. Zhelezniak, et al., Molecules **25**, 4678 (2020). https://doi.org/10.3390/molecules25204678
27. I. A. Zvereva, M. G. Shelyapina, M. Chislov, et al., J. Therm. Anal. Calorim. **147**, 6147 (2022). https://doi.org/10.1007/s10973-021-10947-4
28. D. S. Bogdanov, R. G. Novikov, O. S. Pestsov, et al., Mater. Chem. Phys. **261**, 124235 (2021). https://doi.org/10.1016/j.matchemphys.2021.124235
29. R. I. Yocupicio-Gaxiola, V. Petranovskii, J. Antúnez-García, and S. F. Moyado, Appl. Nanosci. **9**, 557 (2019). https://doi.org/10.1007/s13204-018-0935-1

SPELL: 1. wetted